Line-of-Sight Reconstruction for Faster Homing Guidance

F. William Nesline* and Paul Zarchan†
Raytheon Company, Bedford, Massachusetts

A novel way to generate the signal required for homing guidance is to reconstruct the line-of-sight angle by combining seeker boresight error with an integrated rate gyro signal. The paper shows that line-of-sight (LOS) reconstruction allows reduced stabilization loop gain requirements over other guidance implementations. For a given stabilization loop gain, faster guidance system time constants can be achieved with LOS reconstruction, thus enabling the guidance system to achieve more accurate homing than other implementations.

Introduction

RADAR homing missiles use a space stabilized seeker antenna in order to acquire and track the target. In conventional implementations of proportional navigation guidance systems, the degree to which the seeker is stabilized places fundamental limitations on the homing accuracy of the missile. Imperfect seeker stabilization causes an unwanted feedback path within the missile homing loop. Increasing the guidance time constant is often the only way to satisfy the stability requirements generated by the extra loop. However, increasing the guidance time constant also degrades system performance in terms of increased miss distance due to a maneuvering target.

The purpose of this paper is to explore other implementations of proportional navigation guidance so that faster guidance time constants can be realized in the presence of imperfect seeker stabilization. The paper shows that line-of-sight reconstruction achieves this goal, thus enabling the guidance system to achieve more accurate homing.

Guidance System Alternatives

In a radar homing missile, the seeker boresight error is proportional to the line-of-sight (LOS) rate.[6-8] In conventional implementations of proportional navigation, line-of-sight rate information is required for generating acceleration commands. Since the boresight error signal of the seeker is proportional to the line-of-sight rate,[2,6] the necessary commands can be generated by filtering this signal. For this type of implementation, the seeker stabilization loop gain must be sufficiently large to support the small guidance time constant required for accurate homing.[4,9] If this large stabilization loop gain cannot be attained for practical reasons, the guidance system time constant must be increased, thus increasing the miss distance.

A guidance signal can also be generated by differentiating the boresight error and adding it to the seeker rate gyro output. The paper shows that this implementation, known as LOS rate reconstruction, works well if the missile turning rate time constant is small. If this condition is not met, LOS rate reconstruction requires that either the autopilot time constant, or, if possible, stabilization loop gain, must be increased.

Another method for generating a guidance signal is integration or the output of the seeker rate gyro and adding it to the boresight error. The paper shows that this implementation, known as LOS reconstruction, relaxes stabilization loop requirements, thus allowing faster autopilot time constants for more accurate homing. This method works well even if the missile turning rate time constant is large.

Guidance Signal Reconstruction

Proportional navigation is a method of guidance in which the missile acceleration is made proportional to the line-of-sight rate. The proportional navigation guidance law is an attempt to mechanize an acceleration command, n_c, perpendicular to the line of sight according to

$$n_c = N'V_c\dot{\lambda} \tag{1}$$

where N' is the effective navigation ratio, V_c the closing velocity, and $\dot{\lambda}$ the LOS rate.

In a radar homing missile, the seeker tracks the target. As a consequence the seeker dish rate is approximately the LOS rate. The transfer function of LOS rate to seeker dish rate can be obtained from the geometry of Fig. 1 and is

$$\frac{\dot{D}}{\dot{\lambda}} = \frac{1}{1+T_I S} \tag{2}$$

where T_I is the seeker track loop time constant. Thus we can see that the seeker track loop dynamics causes the dish rate to lag the LOS rate. Since the receiver output or boresight error ϵ is proportional to the seeker dish rate, the LOS rate information is imbedded in the boresight error. In conventional implementations of proportional navigation, the LOS rate estimate, $\hat{\dot{\lambda}}$, is obtained by filtering the boresight error as shown in Fig. 2. The guidance system transfer function can be obtained from Fig. 1 and is

$$\left.\frac{n_c}{\dot{\lambda}}\right|_{\text{CONVENTIONAL}} = \frac{N'V_c}{(1+sT_I)(1+sT_N)} \tag{3}$$

The dynamics associated with the seeker and noise filter will eventually cause miss distance.

Other alternatives exist for generating the signal required for guidance. From Fig. 1 we can see that the LOS angle can be expressed as

$$\lambda = \epsilon + D \tag{4}$$

Therefore, the LOS rate can be obtained by differentiation or

$$\dot{\lambda} = \dot{\epsilon} + \dot{D} \tag{5}$$

Since perfect differentiation is impossible, Eq. (5) must be implemented by using a derivative network to differentiate the boresight error. A simple implementation of LOS rate reconstruction appears in Fig. 3, where the boresight error deriva-

Presented as Paper 83-2170 at the AIAA Guidance and Control Conference, Gatlinburg, Tenn., Aug. 15-17, 1983; received Aug. 24, 1983; revision received Jan. 3, 1984.

*Chief Systems Engineer, Missile Systems Division. Associate Fellow AIAA.

†Principal Engineer, Missile Systems Division. Member AIAA.

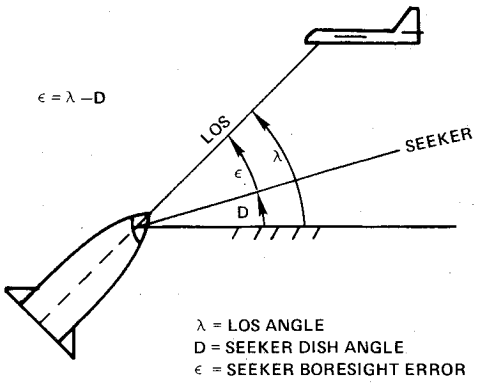

Fig. 1 Seeker geometry.

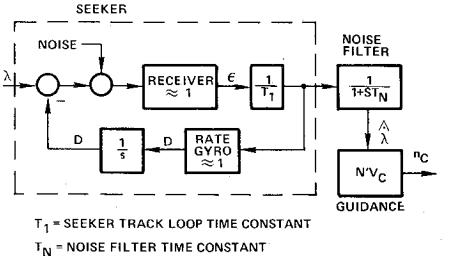

Fig. 2 Conventional implementation of proportional navigation.

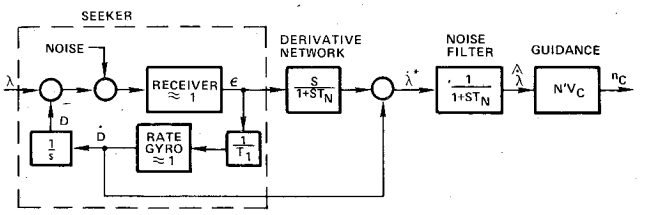

Fig. 3 Proportional navigation via line-of-sight rate reconstruction.

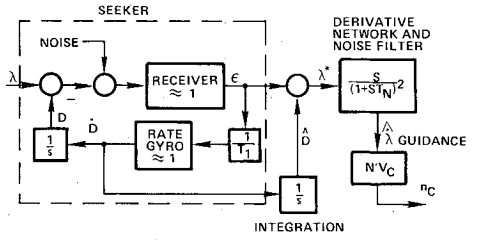

Fig. 4 Proportional navigation via line-of-sight reconstruction.

tive is combined with the rate gyro output. The resultant guidance system transfer function can be obtained from Fig. 3 and is

$$\left.\frac{n_c}{\dot{\lambda}}\right|_{\substack{\text{LOS RATE}\\ \text{CONSTRUCTION}}} = \frac{N'V_c[1+s(T_1+T_N)]}{(1+sT_1)(1+sT_N)^2} \tag{6}$$

In order to avoid differentiation of the noisy boresight error, the guidance signal also can be generated by first reconstructing the LOS angle according to Eq. (4) and then using a simple derivative network and noise filter. A possible implementation of this method, known as LOS reconstruction, appears in Fig. 4. Here the rate gyro output is integrated and added to the boresight error. The guidance transfer function resulting from this method is

$$\left.\frac{n_c}{\dot{\lambda}}\right|_{\substack{\text{LOS}\\ \text{RECONSTRUCTION}}} = \frac{N'V_c}{(1+sT_N)^2} \tag{7}$$

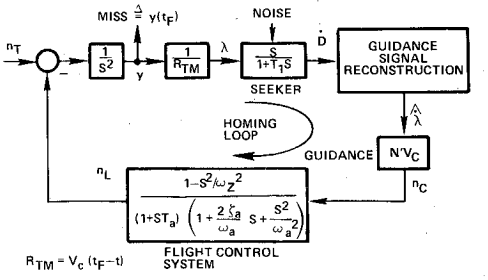

Fig. 5 Simplified planar homing loop.

Table 1 System parameters

Symbol	Definition	Value
V_c	Closing velocity	3000 ft/s
V_M	Missile velocity	2000 ft/s
t_F	Time of flight	10 s
T_1	Seeker track loop time constant	0.1 s
T_N	Noise filter time constant	0.2 s
N'	Effective navigation ratio	3
ω_z	Airframe zero	30 rad/s
T_a	Autopilot time constant	0.1 s
ω_a	Autopilot natural frequency	20 rad/s
ξ_a	Autopilot damping	0.7

Table 2 System error sources

Error source	Value
Random target maneuver	2 g's with starting time uniformly distributed over 10 s
Receiver noise	10 mrad at 30 kft in 100 rad/s bandwidth
Glint noise	10 ft in 12.56 rad/s bandwidth
Range independent noise	1 mrad in 100 rad/s bandwidth

It is interesting to note that in LOS reconstruction, seeker dynamics have been totally eliminated from the guidance transfer function.

Simplified Guidance System Comparison

The planar dynamics of a simplified missile homing loop appear in Fig. 5. This loop is highly idealized, since parasitic effects (unwanted feedback paths) have been neglected. The nonminimum phase zero ω_z of the flight control system is determined by the aerodynamic configuration and is typical of tail-controlled missiles. The flight control system time constant T_a, damping ξ_a, and natural frequency ω_a, are typical parameters in an operational three-loop autopilot. The nominal parameters of the homing loop were listed in Table 1 and typical noise and target maneuver error sources were defined in Table 2.[10] Each of the guidance signal reconstruction methods was evaluated as to its ability to estimate LOS rate both with and without noise present. Figure 6 shows that in the absence of noise, the estimated LOS rates lag the true rates. The lag in estimating the LOS rate is directly related to the guidance transfer functions of Eqs. (3), (6), and (7). All methods yield approximately the same accuracy in estimating LOS rate. However, since the LOS rate reconstruction method yielded faster dynamics for a given noise filter time constant, the estimated LOS rate lagged by less. This benefit resulted in more noise transmission, as can be seen from the LOS rate estimates of Fig. 7. It would appear from these figures that all these methods could be made to have approximately the same performance by judicious selection of the noise filter time constant.

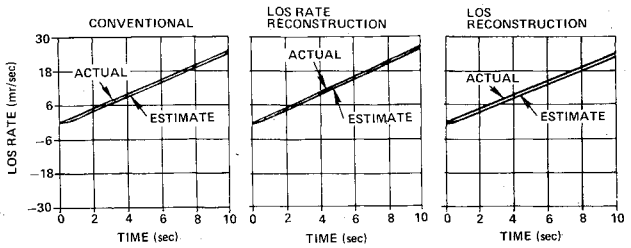

Fig. 6 LOS rate estimates for deterministic case.

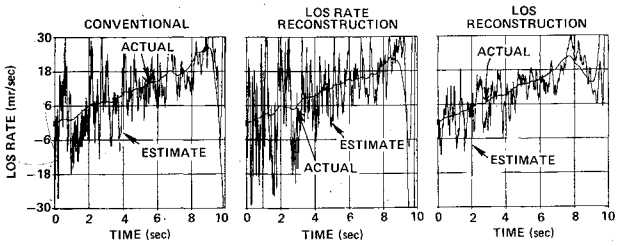

Fig. 7 LOS rate estimates with all error sources.

Guidance System Stability Analysis

In order to compare the guidance signal reconstruction methods more realistically, it is necessary to consider parasitic effects and to perform a stability analysis. A more realistic model of missile system dynamics appears in Fig. 8. Here the

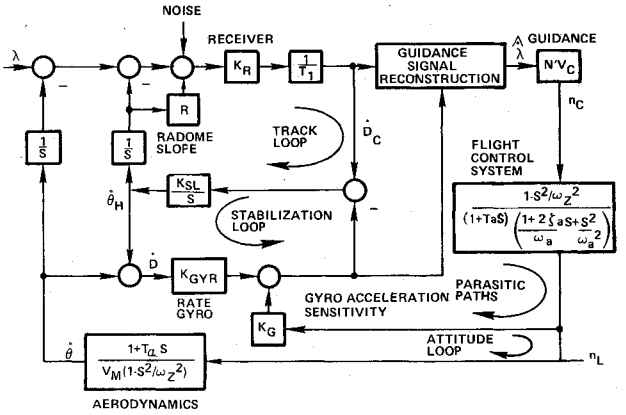

Fig. 8 Missile system dynamics.

seeker contains a tracking loop and simplified stabilization loop. In addition, parameters that represent unwanted, or parasitic, feedback paths for radome refraction slope and for gyro acceleration sensitivity are shown. Receiver and rate gyro scale factor errors are also included in this more realistic model.

An open-loop analysis is conducted by breaking the loop at the acceleration command. Neglecting radome and gyro acceleration sensitivity effects, the open-loop transfer functions can be written for the system employing each of the signal reconstruction methods. They are

$$HG|_{\text{CONVENTIONAL}} = \frac{N'V_c}{K_{SL}V_M}\left[\frac{S(1+T_\alpha s)}{\left(1+\frac{K_{\text{GYR}}T_I}{K_R}s+\frac{s^2T_I}{K_RK_{SL}}\right)(1+sT_N)(1+sT_a)\left(1+\frac{2\xi_a}{\omega_a}s+\frac{s^2}{\omega_a^2}\right)}\right] \tag{8}$$

$$HG\Big|_{\substack{\text{LOS RATE}\\ \text{RECONSTRUCTION}}} = \frac{N'V_cT_I}{V_MK_RK_{SL}}\left[\frac{s^2(K_R-K_{\text{GYR}}-sK_{\text{GYR}}T_N)(1+T_\alpha s)}{\left(1+\frac{K_{\text{GYR}}T_I}{K_R}s+\frac{s^2T_I}{K_RK_{SL}}\right)(1+sT_N)^2(1+sT_a)\left(1+\frac{2\xi_a}{\omega_a}s+\frac{s^2}{\omega_a^2}\right)}\right] \tag{9}$$

$$HG\Big|_{\substack{\text{LOS}\\ \text{RECONSTRUCTION}}} = \frac{N'V_cT_I(K_R-K_{\text{GYR}})}{K_RK_{SL}V_M}\left[\frac{s^2(1+T_\alpha s)}{\left(1+\frac{K_{\text{GYR}}T_I}{K_R}s+\frac{s^2T_I}{K_RK_{SL}}\right)(1+sT_N)^2(1+sT_a)\left(1+\frac{2\xi_a}{\omega_a}s+\frac{s^2}{\omega_a^2}\right)}\right] \tag{10}$$

As can be seen from Eqs. (8-10), all the open-loop transfer functions have different gains and dynamics. These differences become more apparent if there are no receiver and rate gyro scale factor errors ($K_R = K_{\text{GYR}} = 1$). The open-loop transfer functions then become

$$HG\Big|_{\substack{\text{CONVENTIONAL}\\ KR=K\text{GYR}=1}} \approx \frac{N'V_c}{K_{SL}V_M}\left[\frac{s(1+T_\alpha s)}{(1+sT_I)(1+s/K_{SL})(1+sT_N)(1+sT_a)\left(1+\frac{2\xi a}{\omega_a}s+\frac{s^2}{\omega_a^2}\right)}\right] \tag{11}$$

$$HG\Big|_{\substack{\text{LOS RATE}\\ \text{RECONSTRUCTION}\\ KR=K\text{GYR}=1}} \approx \frac{-N'V_cT_IT_N}{V_MK_{SL}}\left[\frac{s^3(1+T_\alpha s)}{(1+sT_I)(1+s/K_{SL})(1+sT_N)^2(1+sT_a)\left(1+\frac{2\xi_a}{\omega_a}s+\frac{s^2}{\omega_a^2}\right)}\right] \tag{12}$$

$$HG\Big|_{\substack{\text{LOS}\\ \text{RECONSTRUCTION}\\ KR=K\text{GYR}=1}} \approx 0 \tag{13}$$

These results indicate that without rate gyro or receiver scale factor errors ($K_{GYR} = K_R = 1$), the open-loop transfer function of the system employing LOS reconstruction is zero. In other words, the seeker appears to be perfectly stabilized. Of course, scale factor errors and parasitic effects will cause imperfect stabilization for LOS reconstruction. Bode plots of Eqs. (10) and (11), utilizing the inputs of Tables 1 and 3, appear in Figs. 9 and 10 respectively. These plots and Eq. (12) indicate that although all systems have adequate stability margins, the best margin is with LOS reconstruction (gain margin = ∞), followed by a conventional system (gain margin = 21.3 dB), and finally LOS rate reconstruction (gain margin = 9.2 dB).

Guidance System Miss Distance Analysis

For the systems under consideration, a miss distance analysis can be conducted via the method of adjoints[11] for the missile system dynamics of Fig. 8 in conjunction with the homing loop of Fig. 11. The results of that analysis are summarized in error budget form in Table 4. This table shows that the total miss distance for all configurations is about the same. The LOS rate reconstruction system is the fastest guidance system (see Figs. 6 and 7) and thus has the lowest miss due to target maneuver and the largest miss due to glint noise. The LOS reconstruction system is the slowest guidance system and thus has the largest miss due to target maneuver and smallest miss due to glint noise. Although all configurations have the same total miss performance, the stability margin for each system is quite different. The margins for all systems will degrade (except LOS reconstruction if $K_R = K_{GYR} = 1$) with increasing turning rate time constant as shown in Fig. 12. If 6 dB of gain margin were required, the maximum allowable turning rate time constant would be about 0.4 s for the LOS rate reconstruction system and about 1.7 s for the conventional system.

Sensitivity to Turning Rate Time Constant

The turning rate time constant, T_α, increases with increasing altitude. Unless specific precautions are taken in the airframe design (i.e., addition of wings), the turning rate time constant could be as large as 2 s. For a 0.1-s autopilot time constant, the stabilization loop gain could be increased to improve the stability margins as shown in Fig. 13. However, this gain cannot be increased without limit because of stability and cost considerations associated with the seeker stabilization loop. If for practical reasons the stabilization loop could be no larger than 100 rad/s, the autopilot time constant would have to be increased to obtain acceptable margins as shown in Fig. 14. The gain margin to strive for in this case would need to be somewhat greater than 6 dB to leave room for the inevitable margin degradation due to receiver and scale factor errors.

If each configuration is designed to yield about 7 dB of margin in the presence of 40% receiver or scale factor errors, we find that the LOS reconstruction system requires 0.1 s autopilot time constant. The conventional system requires 0.3 s, and the LOS rate reconstruction system requires 0.85 s. The stability margin variation with scale factor errors is shown in Fig. 15, while the miss distance error budget associated with each of these designs is presented in Table 5. This table shows that for this turning rate time constant, the superior system is LOS reconstruction. LOS reconstruction achieves the smallest miss distance because its fast autopilot time constant enables it to achieve the smallest miss distance against a maneuvering target.

Sensitivity to Radome Slope

The nonhemispherical shape of the missile radome causes distortion of the incoming radar beam. As the radar beam passes through the radome, a refraction effect takes place, and the net result is an error in the angle of the apparent target. The radome error slope, R, is a measure of the distortion

Table 3 Parameters for missile system dynamics with parasitic paths

Symbol	Definition	Value
R	Radome slope	0.0
K_{SL}	Stabilization loop gain	100.0
K_R	Receiver scale factor	1.0
K_{GYR}	Rate gyro scale factor	1.0
K_G	Gyro acceleration sensitivity	0.0 rad-s/ft
T_α	Turning rate time constant	0.25 s
V_M	Missile velocity	2000 ft/s

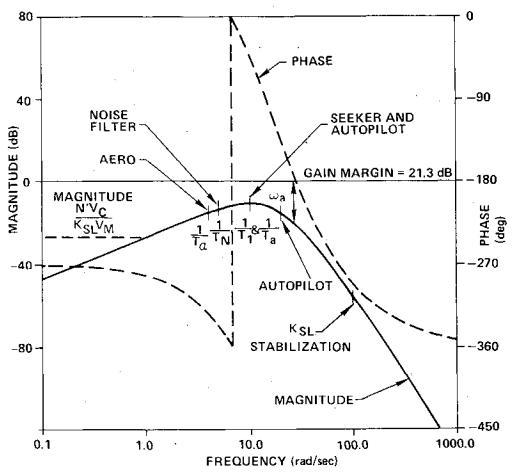

Fig. 9 Bode plot of conventional system ($K_R = K_{GYR} = 1$).

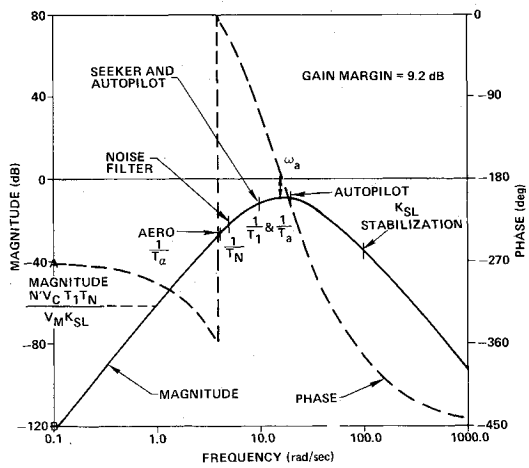

Fig. 10 Bode plot of line-of-sight rate system ($K_R = K_{GYR} = 1$).

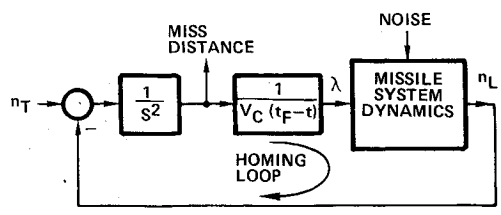

Fig. 11 Miss distance dynamics.

Table 4 Miss distance error budget comparison for $T_\alpha = 0.25$ s

Error source	Value	Conventional, $T_a = 0.1$ s	LOS rate reconstruction, $T_a = 0.1$ s	LOS reconstruction, $T_a = 0.1$ s
Random target maneuver	2 g's uniformly distributed over 10 s	6.4	3.7	9.0
Receiver noise	10 mrad at 30 kft in 100 rad/s bandwidth	1.1	1.1	1.5
Glint noise	10 ft in 12.56 rad/s bandwidth	8.8	10.9	8.4
Range independent noise	1 mrad in 100 rad/s bandwidth	0.8	0.9	0.9
rms miss		10.9 ft	11.6 ft	12.5 ft

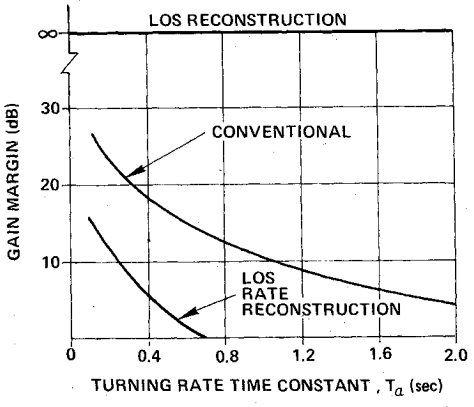

Fig. 12 Stability margins generally degrade with increasing turning rate time constant ($K_R = K_{GYR} = 1$, $T_\alpha = 0.1$ s).

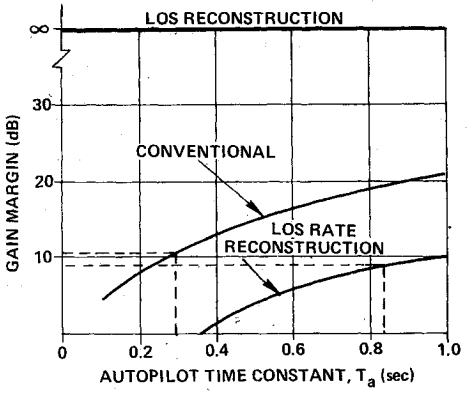

Fig. 14 Stability margins generally improve with increasing autopilot time constant ($K_R = K_{GYR} = 1$, $T_\alpha = 2$ s, $K_{SL} = 100$).

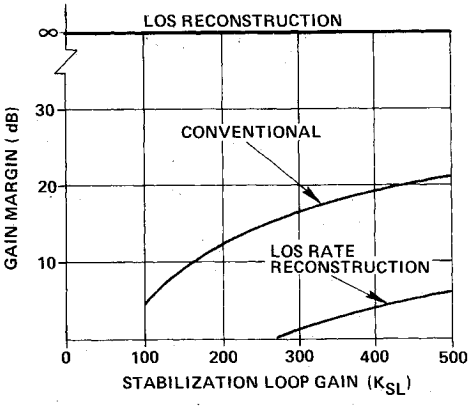

Fig. 13 Stability margins generally improve with increasing stabilization loop gain ($K_R = K_{GYR} = 1$, $T_\alpha = 2$ s, $T_a = 0.1$ s).

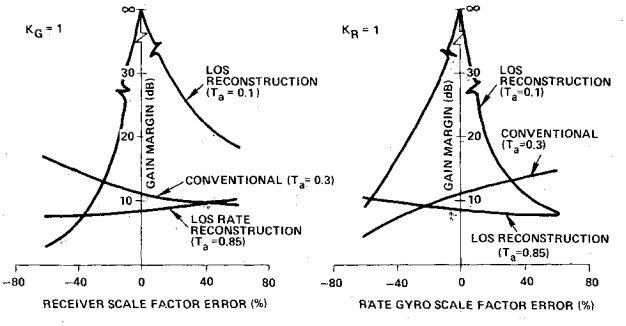

Fig. 15 Each design will yield at least 7 dB of gain margin in the presence of 40% scale factor error.

Table 5 Miss distance error budget comparison for $T_\alpha = 2$ s

Error source	Value	Conventional, $T_a = 0.3$ s	LOS rate reconstruction, $T_a = 0.85$ s	LOS reconstruction, $T_a = 0.1$ s
Random target maneuver	2 g's uniformly distributed over 10 s	16.8	32.9	9.0
Receiver noise	10 mrad at 30 kft in 100 rad/s bandwidth	2.4	2.1	1.5
Glint noise	10 ft in 12.56 rad/s bandwidth	6.9	5.5	8.4
Range independent noise	1 mrad in 100 rad/s bandwidth	1.0	0.7	0.9
rms miss		18.3 ft	33.4 ft	12.5 ft

taking place and is a function of the gimbal angle, among other things. The guidance system designer attempts to specify the manufacturing tolerances and the limits on the permissible variations of R. This error source is particularly important at high altitudes, where the missile turning rate time constant T_α is large. The time constant in conjunction with large radome refraction slopes can cause guidance system instability. The variation of miss distance with radome slope for each configuration is displayed in Fig. 16. Finite stabilization of the seeker ensures that the minimum miss will lie at some negative radome slope. However, since the system employing LOS reconstruction appears to be perfectly stabilized, the minimum miss occurs at zero radome. Figure 16 indicates that each configuration is more sensitive to negative radome slope than to positive slope. For this reason, each system would be biased to allow the most radome slope range. With optimal biasing, the data of Fig. 16 can be redrawn to show how the maximum miss varies with the radome slope range for each configura-

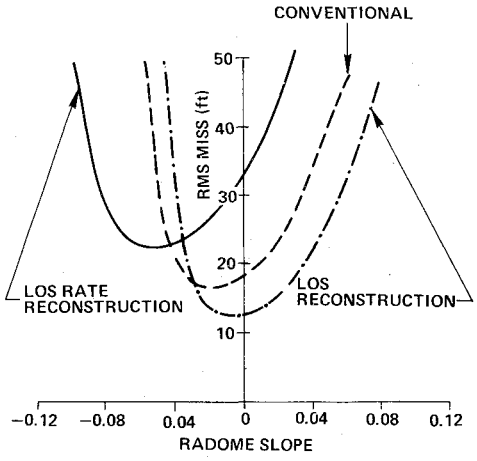

Fig. 16 The performance of all configurations are sensitive to radome slope.

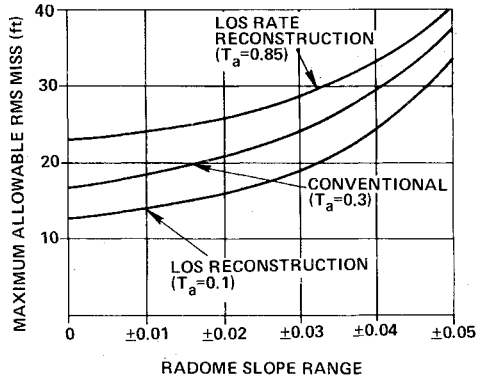

Fig. 17 LOS reconstruction relaxes radome slope requirements.

tion. Figure 17 shows the sensitivity of each configuration to radome slope range. For a given radome slope range, LOS reconstruction yields the minimum miss distance. For comparable performance, LOS rate reconstructions place the most stringent requirements on radome specification, while LOS reconstruction provides the most reduced requirements.

Conclusions

Several radar homing missile implementations of proportional navigation have been explored in terms of their impact on subsystem requirements. When the aerodynamic turning rate time constant is small (i.e., $T_\alpha = 0.25$ s), conventional, LOS rate reconstruction, and LOS reconstruction implementations of proportional navigation allow fast autopilot time constants (i.e., $T_a = 0.1$ s) in the presence of realistic stabilization loop gains (i.e., $K_{SL} = 100$). However, for larger turning rate time constants (i.e., $T_\alpha = 2$ s), only LOS reconstruction allows fast autopilot time constants in the presence of achievable stabilization loop gains. The other guidance implementations require that the autopilot time constant, and, hence, guidance time constant, be increased in order to maintain adequate stability margins [i.e., *gm* (gain margin) = 6 dB]. Thus, for a given stabilization loop gain, faster guidance time constants and smaller miss distances can be achieved with LOS reconstruction.

References

[1]Bryson, A.E. and Ho, Y.C., *Applied Optimal Control*, Blaisdell Publishing Company, Waltham, Mass., 1969 (lecture notes originally published as AIAA Professional Study Series, "Applied Optimal Control," Aug. 1967).

[2]Stallard, D.V., "Classical and Modern Guidance of Homing Interceptor Missiles," presented at Seminar in Department of Aeronautics and Astronautics, MIT, Cambridge, Mass., April 1968.

[3]Garnell, P. and East, D.J., *Guided Weapon Control of Systems*, Pergamon Press, Elmsford, N.Y., 1977.

[4]Travers, P., "Introduction to Interceptor Dynamics," lectures given in Singapore, June 1982.

[5]Nesline, F.W. and Zarchan, P., "A New Look at Classical vs Modern Homing Missile Guidance," *Journal of Guidance and Control*, Vol. 4, Jan.-Feb. 1981, pp. 78-85.

[6]Povejsil, D., Raven, R., and Waterman, P., *Airborne Radar*, D. Van Nostrand Company, Inc., Toronto, 1961.

[7]Nesline, F.W., "Missile Guidance for Low Altitude Air Defense," *Journal of Guidance and Control*, Vol. 2, July-Aug. 1979, pp. 283-289.

[8]Pastrick, H., Seltzer, S., and Warren, M., "Guidance Laws for Short-Range Tactical Missiles," *Journal of Guidance and Control*, Vol. 4, March-April 1981, pp. 98-108.

[9]Nesline, F.W. and Zarchan, P., "Missile Guidance Design Trade-Offs for High Altitude Air Defense," *Journal of Guidance, Control, and Dynamics*, Vol. 6, May-June 1983, pp. 207-212.

[10]Locke, A.S., *Guidance*, D. Van Nostrand, Inc., Toronto, 1955, pp. 608-612.

[11]Zarchan, P., "Complete Statistical Analysis of Nonlinear Missile Guidance Systems—SLAM," *Journal of Guidance and Control*, Vol. 2, Jan.-Feb. 1979, pp. 71-78.